NANO LETTERS

pubs.acs.org/NanoLett Letter

Unconventional Superconducting Diode Effects via Antisymmetry and Antisymmetry Breaking

Chong Li,[▽] Yang-Yang Lyu,[▽] Wen-Cheng Yue,[▽] Peiyuan Huang, Haojie Li, Tianyu Li, Chen-Guang Wang, Zixiong Yuan, Ying Dong, Xiaoyu Ma, Xuecou Tu, Tao Tao, Sining Dong,* Liang He, Xiaoqing Jia, Guozhu Sun, Lin Kang, Huabing Wang,* Francois M. Peeters, Milorad V. Milošević,* Peiheng Wu, and Yong-Lei Wang*

Cite This: *Nano Lett.* 2024, 24, 4108−4116 Read Online

ACCESS | Metrics & More | Article Recommendations | Supporting Information

ABSTRACT: Symmetry breaking plays a pivotal role in unlocking intriguing properties and functionalities in material systems. For example, the breaking of spatial and temporal symmetries leads to a fascinating phenomenon: the superconducting diode effect. However, generating and precisely controlling the superconducting diode effect pose significant challenges. Here, we take a novel route with the deliberate manipulation of magnetic charge potentials to realize unconventional superconducting flux-quantum diode effects. We achieve this through suitably tailored nanoengineered arrays of nanobar magnets on top of a superconducting thin film. We demonstrate the vital roles of inversion antisymmetry and its breaking in evoking unconventional superconducting effects, namely a magnetically symmetric diode effect and an odd-parity magnetotransport effect. These effects are nonvolatilely controllable through in situ magnetization switching of the nanobar magnets. Our findings promote the use of antisymmetry (breaking) for initiating unconventional superconducting properties, paving the way for exciting prospects and innovative functionalities in superconducting electronics.

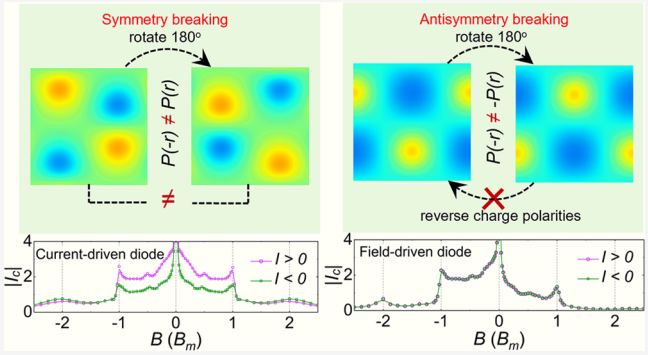

KEYWORDS: *superconducting diode, inversion antisymmetry, antisymmetry breaking, odd-parity magnetotransport, vortex*

Generally, the charge transport effect in a material exhibits even symmetry with respect to the externally applied electric current and magnetic field.[1] For instance, the resistance typically remains unchanged between reversed currents and between inverted magnetic fields. Recently, the superconducting diode effect with one-way supercurrent has gathered significant attention due to its potential for dissipationless electronics.[2−20] Such a diode shows zero resistance when current flows in one direction while exhibiting normal resistance when the current is reversed. Its manifestation typically relies on the simultaneous breaking of space inversion and time reversal symmetry.[2−15] Notably, the polarity of the diode can be reversed by inverting the applied magnetic field.[2−15] This phenomenon is generally described by the magnetochiral anisotropy, which incorporates a nonlinear resistance term ($\gamma \boldsymbol{B}\cdot\boldsymbol{I}$) that is dependent on both the applied electric current I and the magnetic field B (γ denotes the magnetochiral anisotropy coefficient).[2−6] Consequently, a superconducting diode often exhibits a simultaneous nonreciprocal effect in response to both electric currents and magnetic fields. The intricate connections between the superconducting nonreciprocal charge transport and the symmetry breaking remain ambiguous, limiting the deliberate control of superconducting diodes.

On the other hand, a special type of superconducting diodes, relying on ratchet motion of superconducting flux-quanta, has been extensively investigated for years.[21−35] In type-II superconductors, magnetic flux penetrates the material in the form of individual flux-quanta (also known as vortices). The motion of such flux-quanta directly impacts the electromagnetic properties of superconductors.[36] Introducing symmetry breaking in the pinning potentials leads to the one-way motion of flux-quanta, thus presenting a flux-quantum diode.[21−34] However, akin to other superconducting diodes, the vast majority of previously reported flux-quantum diodes also display asymmetric responses with respect to both I and B,[21−30] consistent with the description by magnetochiral

Received: December 19, 2023
Revised: March 20, 2024
Accepted: March 20, 2024
Published: March 27, 2024

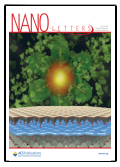

Downloaded via NANJING UNIV on July 6, 2024 at 10:38:35 (UTC).
See https://pubs.acs.org/sharingguidelines for options on how to legitimately share published articles.

ACS Publications © 2024 American Chemical Society

https://doi.org/10.1021/acs.nanolett.3c05008
Nano Lett. 2024, 24, 4108−4116

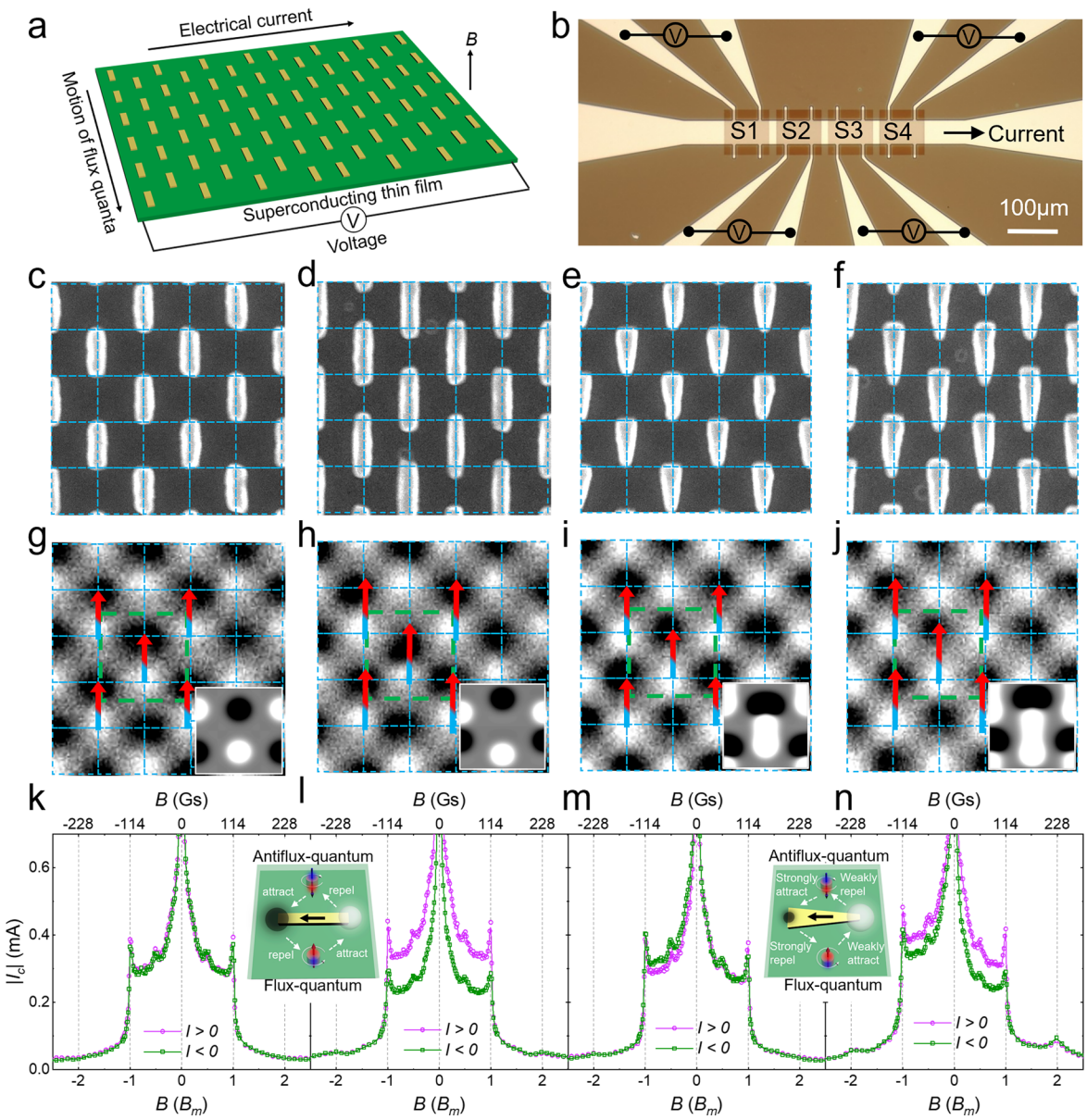

Figure 1. Unconventional flux-quantum diode effects. (a) Schematic diagram illustrating an array of nanomagnets on top of a superconducting film. (b) Optical image of a superconducting MoGe microbridge with four sections (S1−S4) patterned with square arrays of nanomagnets, shown in (c−f), respectively. Scale bar, 100 μm. (c−f) Scanning electron microscopy (SEM) images showing square arrays of nanomagnet structures. The square lattice constant is 300 nm. (g−j) MFM images of the nanomagnet arrays in (c−f). The black and white spots reveal positive and negative magnetic charges, respectively, while the arrows indicate the magnetizations of the single-domain nanomagnets. The insets display the images obtained from micromagnetic simulations. (k−n) Comparisons of critical current curves for positive and negative currents from the four sections S1−S4, respectively. The insets display the interactions between a nanomagnet and a flux-quantum (bottom) and an antiflux-quantum (top).

anisotropy.[2−6] So far, whether magnetochiral anisotropy plays a center role in superconducting diodes is still an open question.

In this study, we demonstrate, both experimentally and numerically, the creation and manipulation of two types of unconventional superconducting diode effects that cannot be described by magnetochiral anisotropy. We showcase a magnetically symmetric superconducting diode with a substantial diode efficiency of up to 20%, as well as an electrically symmetric superconducting odd-parity magneto-transport effect, presenting a unique superconducting diode driven by magnetic fields instead of electric currents. We achieve the first unconventional diode effect by introducing a spatial inversion antisymmetric magnetic potential in the system; then, we break the antisymmetry to realize the later one. These unique novel diode effects are produced in sophisticatedly designed hybrid devices containing arrays of nanobar magnets on top of a superconducting thin film, as illustrated in Figure 1a.

Our device consists of a microbridge (50 nm in thickness and 50 μm in width) of amorphous superconducting $Mo_{0.79}Ge_{0.21}$ (MoGe) (Figure 1b), known for its weak intrinsic pinning, thus enabling the access of emergent effects from artificially introduced potential landscapes.[37,38] The superconducting critical temperature of our microstripe is 7.15 K (Figure S2). The microbridge comprises four sections (S1−S4), each with square arrays of nanomagnets with different sizes and geometries (Figure 1c−f) to demonstrate various

https://doi.org/10.1021/acs.nanolett.3c05008
Nano Lett. 2024, 24, 4108−4116

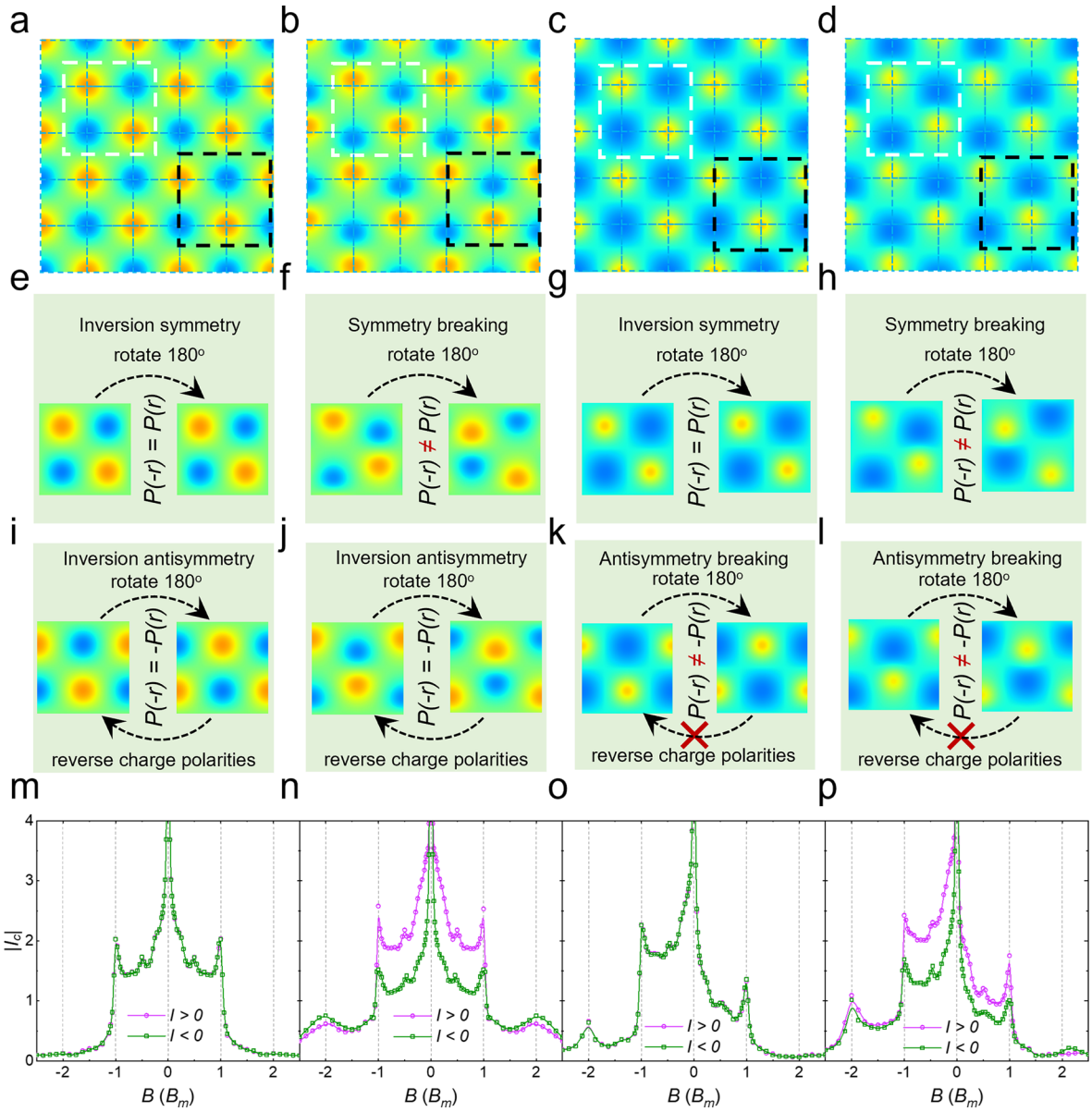

Figure 2. Theoretical models and numerical simulations of unconventional diode effects. (a−d) Models of magnetic charge potentials corresponding to Figure 1g−j, respectively. The blue and red spots represent attractive and repulsive pinning potentials to flux-quanta, respectively. White and black boxes highlight the unit cells of the same size as described in (e−h) and (i−l), respectively. (e−h) Illustrations of space inversion symmetry and its breaking. (i−l) Illustrations of space inversion antisymmetry and its breaking. (m−p) MD simulations of $|I_c| \sim B$ curves using the potentials in (a−d), respectively.

superconducting effects. The detailed device fabrication procedures and parameters can be found in the Supporting Information. Each nanobar magnet can be considered as a pair of magnetic charges, one positive and one negative, respectively repelling and attracting the flux-quantum (inset of Figure 1l).[34,39] The magnetic charge patterns of the nanomagnet arrays are directly observed through magnetic force microscopy (MFM) imaging, as shown in Figure 1g−j.

First, we present the generation of a distinctive superconducting diode that cannot be described by magnetochiral anisotropy. Figure 1k−n displays the B-dependent critical currents I_c under positive (purple curve) and negative (green curve) currents from microbridge sections S1−S4, respectively. The I_c curves are extracted from the B- and I-dependent dissipation voltage maps (Figure S3). Clear peaks appear in all curves at the matching magnetic field B_m= 114 Gs, corresponding to the flux-quantum density of one flux-quantum per nanomagnet. This indicates strong magnetic pinning provided by the nanomagnet arrays to the flux-quanta. In Figure 1k, the I_c curves for microbridge S1 are symmetric with respect to both I and B. This results from the length of the rectangular nanomagnets in microbridge S1 matching the square lattice constant of 300 nm (Figure 1c), thereby generating a symmetric magnetic charge pattern, as depicted in Figure 2a,e. To break the space inversion symmetry, we elongate the nanomagnets in microbridge S2 (Figure 1d), where the nanomagnet length of 400 nm is longer than the square lattice constant. This alteration breaks the space inversion symmetry (Figure 2b,f). Consequently, a significant discrepancy between the I_c curves for positive and negative currents is observed (Figure 1l), leading to a flux-quantum diode effect. This current-driven nonreciprocal effect arises

https://doi.org/10.1021/acs.nanolett.3c05008
Nano Lett. 2024, 24, 4108−4116

directly from the breaking of space inversion symmetry in the pinning potential.[21−33,39−42] In our case, the symmetry breaking occurs from the asymmetric distribution of positive and negative magnetic charges (Figure 2f). The observed flux-quantum diode demonstrates a substantial superconducting diode efficiency ($[|I_c(+) - I_c(-)|]/[I_c(+) + I_c(-)]$) of up to 20% over a wide magnetic field range (Figure S4).

Unlike traditional superconducting diodes, which typically display simultaneous nonreciprocal transport in response to both I and B,[2−15,21−30,43,44] the superconducting diode shown in Figure 1l exhibits a symmetric response to magnetic field $\boldsymbol{B}$, contrary to the principle of magnetochiral anisotropy. To unveil the underlining mechanism behind this unconventional superconducting diode effect, we analyze the symmetry of magnetic charges and their interaction with flux-quanta. In addition to the symmetry breaking (Figure 2f), we find the magnetic charge pattern also displays inversion antisymmetry (Figure 2j). The antisymmetry plays a pivotal role in the magnetically symmetric transport properties within our devices, as elaborated below.

The inversion antisymmetry (Figure 2j) is described by

$$P(-r) = -P(r) \tag{1}$$

where $P \rightarrow -P$ represents the inversion of magnetic charge potentials (positive to negative and vice versa) and $r \rightarrow -r$ denotes the space inversion operation. Furthermore, the interactions between magnetic charges and flux-quanta are opposite to those between identical magnetic charges and antiflux-quanta, as shown in the inset of Figure 1l. This relationship is denoted by

$$P(-B) = -P(B) \tag{2}$$

where $P(B)$ and $P(-B)$ represent the magnetic pinning potentials from the same charge pattern for flux-quanta and antiflux-quanta, respectively. Additionally, considering a given pinning potential P, the following relationships hold (refer to Figures S5 and S6 for details):

$$\begin{cases} V(-B, -I, P) = -V(B, I, P) & (3) \\ V[B, -I, P(-r)] = -V[B, I, P(r)] & (4) \end{cases}$$

where V represents the dissipation voltage, directly measuring the motion of (anti)flux-quanta. Due to negative resistance being forbidden, a sign reversal of V is necessary whenever the polarity of the applied current I is changed. Equation 3 states that the energy dissipation of flux-quanta while moving across a specific pinning potential equals that of antiflux-quanta (driven by reversed current) within the same pinning potential (Figure S5). Equation 4 indicates that the motion of flux-quanta across a pinning potential, under the space inversion operation, is equivalent to their motion under a reversed driving current across the original potential (Figure S6). Combining eqs 1−4 yields

$$V(-B) = V(B)$$

Hence, this suggests that space inversion antisymmetry leads to symmetric transport responses against the out-of-plane magnetic field $\boldsymbol{B}$, thus giving rise to a unique superconducting diode. This unconventional diode effect can be accurately replicated by our molecular dynamic (MD) simulations shown in Figure 2n and visually demonstrated in Video S1. Snapshots captured from the video are presented in Figure S7. Notably, the flux-quanta move only for one polarity of the current, clearly revealing a current-driven diode effect.

The above analysis highlights the significant role of antisymmetry in achieving a magnetically symmetric diode effect. To explore the emergent effect from antisymmetry breaking, we design a distinctive nanomagnet array using asymmetric nanobars (Figure 1e). Both MFM imaging (Figure 1i) and micromagnetic simulations (inset of Figure 1i) reveal differences in the spatial spread and stray field strength of magnetic charges at the two ends of the asymmetric magnetic nanobar. The narrower end exhibits a more widely spread magnetic charge compared to the wider end, as depicted in the inset of Figure 1n. Since the positive and negative charges from the same nanomagnet produce equal total flux, the focused charge generates a more localized yet stronger pinning force in contrast to the widely spread charge (inset of Figure 1n). These mismatches in magnetic potentials between positive and negative charges break the inversion antisymmetry of pinning potentials, signified by $P(-r) \neq -P(r)$ (illustrated in Figure 2k).

Both our experimental (Figure 1m) and MD simulation (Figure 2o) results reveal an asymmetric response to the magnetic field. The I_c at the negative fields (within the matching magnetic field) surpasses that at positive fields. This discrepancy gives rise to an odd-parity component of I_c, represented as $I_c^{odd} = [|I_c(B)| - |I_c(-B)|]/2$, showcasing a superconducting odd-parity magnetotransport effect.

Odd-parity magnetotransport is a rare phenomenon, observed in exceptional cases where time reversal symmetry is broken within a few material systems.[45−49] This uncommon field-driven nonreciprocal effect is typically subtle.[46−49] A recent study highlighted a substantial odd-parity magnetoresistance in an InAs quantum well,[45] emphasizing this intriguing effect in nonsuperconducting materials. While in superconductors, the odd-parity magnetotransport effect has been numerically explored in Josephson junctions subjected to a local inhomogeneous magnetic field,[50] experimental demonstrations of such unconventional superconducting effect are scarce. Our work presents an effective method for experimentally triggering this unconventional superconducting effect through antisymmetry breaking.

Although asymmetric magnetic field responses have been widely demonstrated in superconducting diodes,[2−15,21−30] satisfying magnetochiral anisotropy, these diodes exhibit a simultaneous current-driven nonreciprocal effect known as the regular diode effect. However, our observed superconducting odd-parity magnetotransport effect displays symmetric responses regarding electric currents. As shown in Figures 1m and 2o, the I_c curves under positive and negative currents overlap. Hence, this electrically symmetric yet magnetically asymmetric superconducting effect also rules out the mechanism of magnetochiral anisotropy. This sets apart the superconducting odd-parity magnetotransport effect induced by antisymmetry breaking from any previously reported superconducting diode effects satisfying magnetochiral anisotropy,[2−15,21−30] typically induced by standard spatial-temporal symmetry breaking. The electrically symmetric response observed in microbridge S3 occurs because the length of the asymmetric nanobar matches the square lattice constant of 300 nm; hence, the antisymmetric magnetic charge pattern preserves the inversion symmetry (Figure 2g).

The odd-parity magnetotransport effect is visualized in the MD simulation in Video S2. Snapshots captured from the

https://doi.org/10.1021/acs.nanolett.3c05008
Nano Lett. 2024, 24, 4108−4116

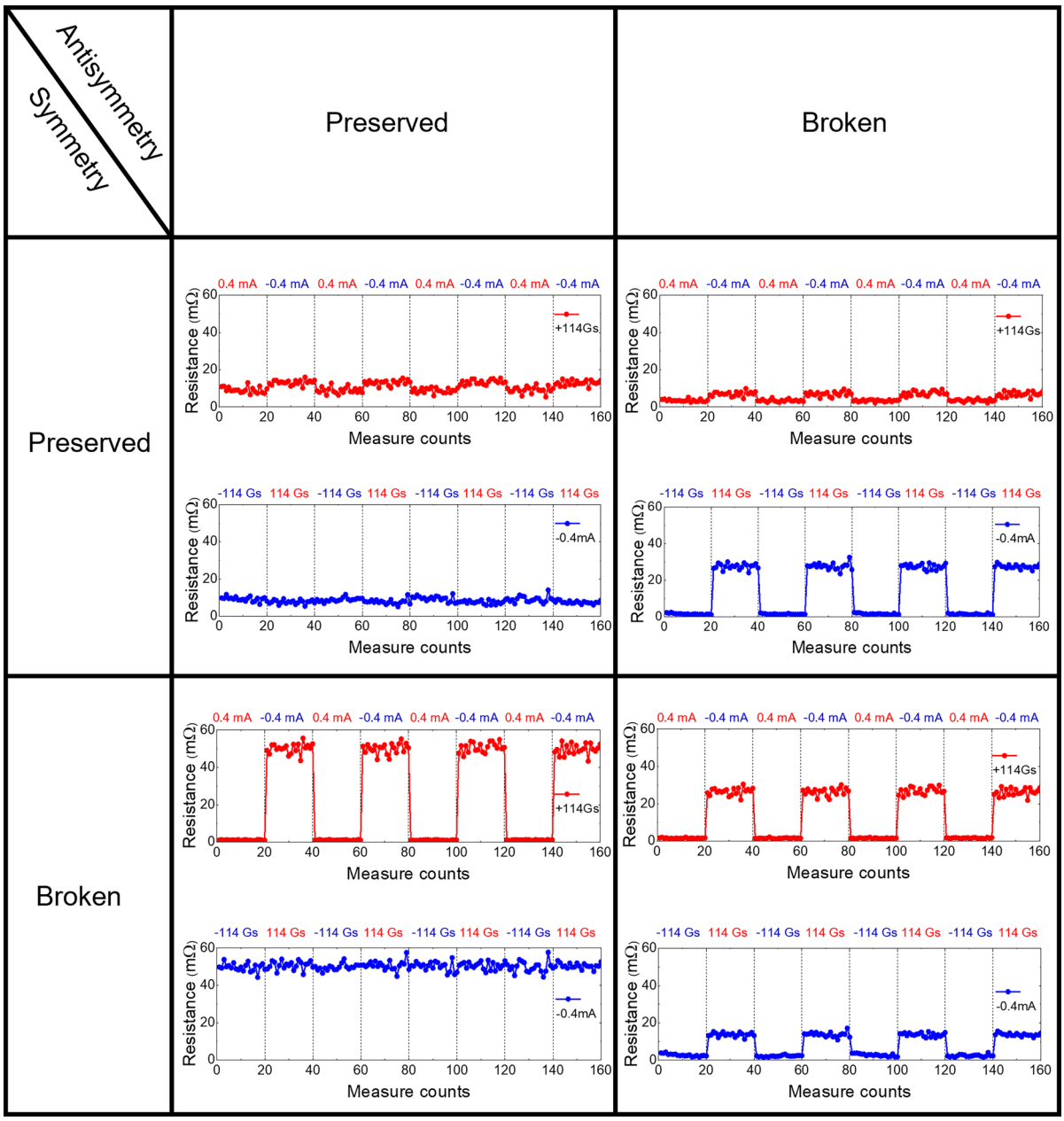

Figure 3. Switchable superconductivity. The red and blue curves display the resistance switching by alternatively reversing electric currents (red) and magnetic fields (blue).

video are presented in Figure S8. Notably, the flux-quanta move solely for one polarity of the applied magnetic fields. This behavior resembles that of a current-driven flux-quantum diode, where flux-quantum moves exclusively for only one polarity of applied current, suggesting a magnetic-field-driven diode effect.

We can merge both the current-driven diode effect and the magnetic-field-driven diode effect into one device by simultaneously breaking inversion symmetry and antisymmetry. This can be achieved by extending the length of the asymmetric nanomagnets, as depicted in Figure 1f. The corresponding magnetic charge pattern (shown in Figures 1j and 2d) reveals simultaneous symmetry breaking (Figure 2h) and antisymmetry breaking (Figure 2l). As anticipated, the I_c curves (Figure 1n in the experiment and Figure 2p in the simulation) display asymmetry concerning both I and B, resembling the behavior of a traditional superconducting diode.

However, different from the traditional superconducting diodes where the diode polarity can be inverted by changing the direction of the magnetic field, in Figure 1n, the diode polarity remains the same between positive and negative magnetic fields despite a clear asymmetric magnetic field dependence. This discrepancy arises because reversing the current does not alter the pinning strengths determined by the magnetic charges, although it does reverse the flow direction of flux-quanta.

To further demonstrate the deliberate unconventional superconducting diode effects, we showcase the effects of the switching current and magnetic field in Figure 3. The red curves display the resistance switching effect upon alternatively reversing electric currents, while the blue curves display the

https://doi.org/10.1021/acs.nanolett.3c05008
Nano Lett. 2024, 24, 4108−4116

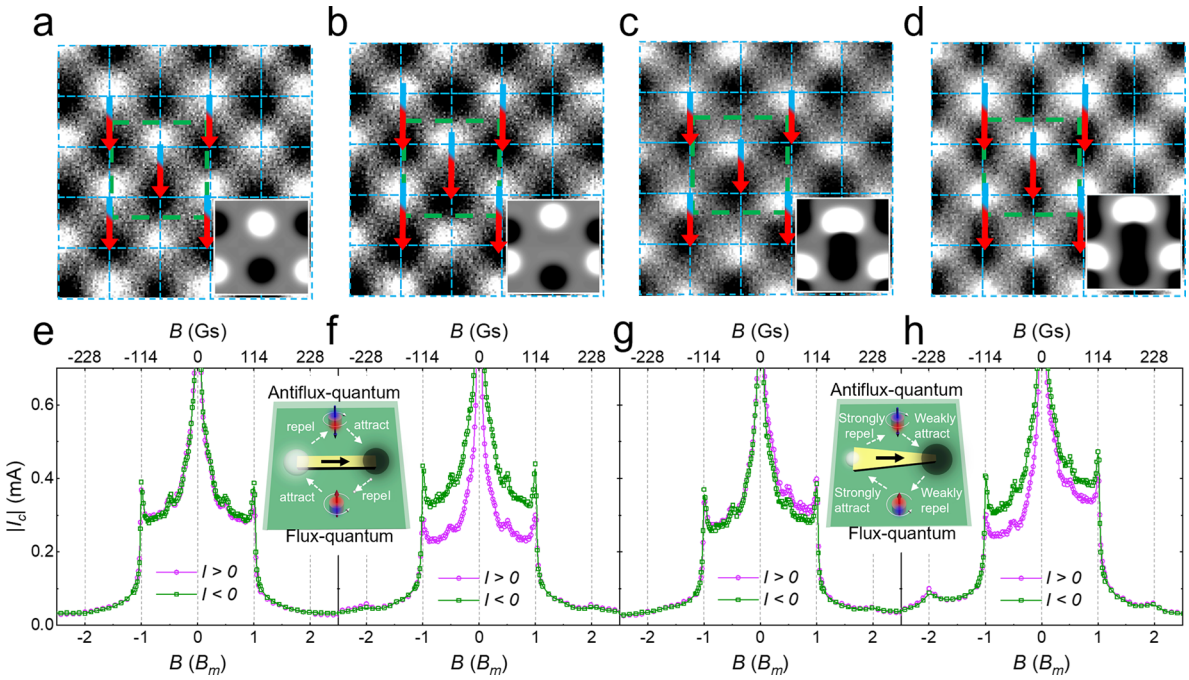

Figure 4. Reversing diode polarities. (a−d) MFM images of the nanomagnet arrays (Figure 1c−f) under reversed magnetization. Insets are images from micromagnetic simulations. (e−h) Experimental $I_c \sim B$ curves corresponding to (a−d), respectively. The insets illustrate the reversed interactions between the nanomagnets and (anti)flux-quantum.

switching effect upon alternatively reversing magnetic fields. The results can be categorized into four groups based on the parity operation of inversion symmetry and antisymmetry: (1) no diode switching effects occur under simultaneously preserved inversion symmetry and antisymmetry. (2) Pure current-driven diode switching occurs when inversion symmetry is violated while antisymmetry is preserved. (3) Pure magnetic-field-driven diode switching occurs when antisymmetry is violated while inversion symmetry is preserved. (4) Both current- and magnetic-field-driven diode switching occurs when both inversion symmetry and antisymmetry are violated. These results suggest that magnetic symmetry breaking solely governs the current-driven diode effect, while antisymmetry breaking solely governs the magnetic-field-driven diode (or odd-parity magnetotransport) effect. Notably, all these unconventional superconducting effects cannot be described by a magnetochiral anisotropy picture.

In traditional superconducting diodes,[2−15,21−30] the reversal of the nonreciprocal effect against current (or magnetic field) could be achieved by changing the direction of the magnetic field (or current), as required by magnetochiral anisotropy. However, as mentioned above, all nonreciprocal effects in our devices both electrically and magnetically violate the principle of magnetochiral anisotropy. Consequently, their polarities cannot be altered by switching currents or magnetic fields.

However, we can reverse the diode polarity through a novel and nonvolatile method by inverting the magnetization states of the nanomagnets. This inversion can be achieved through in situ-applied in-plane magnetic fields. As depicted in Figure 4a−d, when the magnetization state of the nanomagnets is inverted, the polarities of the magnetic charges switch, while their distributions and strengths remain unchanged. This inverts the orientations of symmetry breaking and antisymmetry breaking, consequently reversing the polarities for all electric and magnetic nonreciprocal effects (as shown in Figure 4e−h). The reversed diode effects are also replicated by our molecular dynamic (MD) simulations (Figure S9).

We have successfully demonstrated how the introduction and subsequent breaking of space inversion antisymmetry in magnetic charge potentials can unlock unconventional properties within superconductors. Specifically, by incorporating space inversion antisymmetry, we have facilitated the emergence of a magnetically symmetric superconducting diode. More intriguingly, intentionally disrupting this antisymmetry has proven to be an effective strategy for activating the odd-parity magnetotransport effect, leading to a unique magnetic-field-driven superconducting diode. A schematic phase diagram of major superconducting responses in regard to symmetry (breaking) and antisymmetry (breaking) is displayed in Figure S10. It should be noted that our results unambiguously rule out the role of magnetochiral anisotropy in our superconducting diodes.

These findings serve as a conceptual proof-of-principle and invite further exploration of emergent properties associated with inversion antisymmetry and its breaking, holding the potential for application across diverse material systems hosting (quasi)particles beyond superconducting flux-quanta. For instance, this can be extended to magnetic colloids,[51,52] skyrmions,[53] and magnetic vortices,[54] where the polarities of these particles can also be controlled by magnetic fields. Moreover, by extending this manipulation to electric (quasi)-particles, the introduction of unique electric potentials with antisymmetry or their breaking could lead to innovative transport phenomena. This could be realized by fabricating nanopatterned gating electrodes in two-dimensional materials like graphene,[55] where the charge polarities (electrons and holes) can be controlled using an electric field. Hence, the future exploratory use of inversion antisymmetry and its

https://doi.org/10.1021/acs.nanolett.3c05008
Nano Lett. 2024, 24, 4108−4116

breaking holds great potential for discovering new principles and functionalities, paving the way for innovative applications.

■ ASSOCIATED CONTENT

Supporting Information

The Supporting Information is available free of charge at https://pubs.acs.org/doi/10.1021/acs.nanolett.3c05008.

Methods for sample fabrication, experiments, molecular dynamic simulations and micromagnetic simulations, and Figures S1−S10 (PDF)

Video S1: MD simulation for unconventional superconducting vortex diode effects with inversion antisymmetry (MP4)

Video S2: MD simulation for unconventional superconducting vortex diode effects with antisymmetry breaking (MP4)

■ AUTHOR INFORMATION

Corresponding Authors

Sining Dong − *Research Institute of Superconductor Electronics, School of Electronic Science and Engineering, Nanjing University, Nanjing 210023, China; National Key Laboratory of Spintronics, Nanjing University, Suzhou 215163, China;* orcid.org/0000-0002-1109-5602; Email: sndong@nju.edu.cn

Huabing Wang − *Research Institute of Superconductor Electronics, School of Electronic Science and Engineering, Nanjing University, Nanjing 210023, China; Purple Mountain Laboratories, Nanjing 211111, China;* orcid.org/0000-0003-4802-6077; Email: hbwang@nju.edu.cn

Milorad V. Milošević − *Department of Physics, University of Antwerp, B-2020 Antwerp, Belgium; Instituto de Física, Universidade Federal de Mato Grosso, Cuiaba, Mato Grosso 78060-900, Brazil;* orcid.org/0000-0002-5431-377X; Email: milorad.milosevic@uantwerpen.be

Yong-Lei Wang − *Research Institute of Superconductor Electronics, School of Electronic Science and Engineering, Nanjing University, Nanjing 210023, China; Purple Mountain Laboratories, Nanjing 211111, China; National Key Laboratory of Spintronics, Nanjing University, Suzhou 215163, China;* orcid.org/0000-0003-0391-7757; Email: yongleiwang@nju.edu.cn

Authors

Chong Li − *Research Institute of Superconductor Electronics, School of Electronic Science and Engineering, Nanjing University, Nanjing 210023, China; Purple Mountain Laboratories, Nanjing 211111, China*

Yang-Yang Lyu − *Research Institute of Superconductor Electronics, School of Electronic Science and Engineering, Nanjing University, Nanjing 210023, China; Purple Mountain Laboratories, Nanjing 211111, China*

Wen-Cheng Yue − *Research Institute of Superconductor Electronics, School of Electronic Science and Engineering, Nanjing University, Nanjing 210023, China; Purple Mountain Laboratories, Nanjing 211111, China*

Peiyuan Huang − *Research Institute of Superconductor Electronics, School of Electronic Science and Engineering, Nanjing University, Nanjing 210023, China*

Haojie Li − *Research Institute of Superconductor Electronics, School of Electronic Science and Engineering, Nanjing University, Nanjing 210023, China*

Tianyu Li − *Research Institute of Superconductor Electronics, School of Electronic Science and Engineering, Nanjing University, Nanjing 210023, China*

Chen-Guang Wang − *Research Institute of Superconductor Electronics, School of Electronic Science and Engineering, Nanjing University, Nanjing 210023, China; Purple Mountain Laboratories, Nanjing 211111, China*

Zixiong Yuan − *Research Institute of Superconductor Electronics, School of Electronic Science and Engineering, Nanjing University, Nanjing 210023, China*

Ying Dong − *College of Metrology & Measurement Engineering, China Jiliang University, Hangzhou 310018, China*

Xiaoyu Ma − *Microsoft, Redmond, Washington 98052, United States*

Xuecou Tu − *Research Institute of Superconductor Electronics, School of Electronic Science and Engineering, Nanjing University, Nanjing 210023, China*

Tao Tao − *National Key Laboratory of Spintronics, Nanjing University, Suzhou 215163, China*

Liang He − *National Key Laboratory of Spintronics, Nanjing University, Suzhou 215163, China;* orcid.org/0000-0002-5279-0097

Xiaoqing Jia − *Research Institute of Superconductor Electronics, School of Electronic Science and Engineering, Nanjing University, Nanjing 210023, China*

Guozhu Sun − *Research Institute of Superconductor Electronics, School of Electronic Science and Engineering, Nanjing University, Nanjing 210023, China; Purple Mountain Laboratories, Nanjing 211111, China*

Lin Kang − *Research Institute of Superconductor Electronics, School of Electronic Science and Engineering, Nanjing University, Nanjing 210023, China*

Francois M. Peeters − *Department of Physics, University of Antwerp, B-2020 Antwerp, Belgium; Departamento de Física, Universidade Federal do Ceará, 60455-900 Fortaleza, Ceará, Brazil;* orcid.org/0000-0003-3507-8951

Peiheng Wu − *Research Institute of Superconductor Electronics, School of Electronic Science and Engineering, Nanjing University, Nanjing 210023, China; Purple Mountain Laboratories, Nanjing 211111, China*

Complete contact information is available at: https://pubs.acs.org/10.1021/acs.nanolett.3c05008

Author Contributions

[▽]C.L., Y.-Y.L., and W.-C.Y. contributed equally to this work.

Notes

The authors declare no competing financial interest.

■ ACKNOWLEDGMENTS

This work was supported by the National Natural Science Foundation of China (62288101, 62274086, and 12204434), the National Key R&D Program of China (2021YFA0718802 and 2023YFF0718400), the Fundamental Research Funds for the Central Universities, the Jiangsu Key Laboratory of Advanced Techniques for Manipulating Electromagnetic Wavesm and the Research Foundation-Flanders (FWO-Vlaanderen).

REFERENCES

(1) Onsager, L. Reciprocal relations in irreversible processes. *I. Phys. Rev.* **1931**, *37*, 405−426.

(2) Ando, F.; Miyasaka, Y.; Li, T.; Ishizuka, J.; Arakawa, T.; Shiota, Y.; Moriyama, T.; Yanase, Y.; Ono, T. Observation of superconducting diode effect. *Nature* **2020**, *584*, 373.

(3) Miyasaka, Y.; Kawarazaki, R.; Narita, H.; Ando, F.; Ikeda, Y.; Hisatomi, R.; Daido, A.; Shiota, Y.; Moriyama, T.; Yanase, Y.; Ono, T. Observation of nonreciprocal superconducting critical field. *Appl. Phys. Express* **2021**, *14*, No. 073003.

(4) Baumgartner, C.; Fuchs, L.; Costa, A.; Reinhardt, S.; Gronin, S.; Gardner, G. C.; Lindemann, T.; Manfra, M. J.; Faria Junior, P. E.; Kochan, D.; Fabian, J.; Paradiso, N.; Strunk, C. Supercurrent rectification and magnetochiral effects in symmetric Josephson junctions. *Nat. Nanotechnol.* **2022**, *17*, 39.

(5) Bauriedl, L.; Bäuml, C.; Fuchs, L.; Baumgartner, C.; Paulik, N.; Bauer, J. M.; Lin, K.-Q.; Lupton, J. M.; Taniguchi, T.; Watanabe, K.; Strunk, C.; Paradiso, N. Supercurrent diode effect and magnetochiral anisotropy in few-layer NbSe2. *Nat. Commun.* **2022**, *13*, 4266.

(6) Nadeem, M.; Fuhrer, M. S.; Wang, X. Superconducting diode effect − Fundamental Concepts, Material Aspects, and Device Prospects. *arXiv* **2023**, 1.

(7) Lyu, Y.-Y.; Jiang, J.; Wang, Y.-L.; Xiao, Z.-L.; Dong, S.; Chen, Q.-H.; Milošević, M. V.; Wang, H.; Divan, R.; Pearson, J. E.; Wu, P.; Peeters, F. M.; Kwok, W.-K. Superconducting diode effect via conformal-mapped nanoholes. *Nat. Commun.* **2021**, *12*, 2703.

(8) Turini, B.; Salimian, S.; Carrega, M.; Iorio, A.; Strambini, E.; Giazotto, F.; Zannier, V.; Sorba, L.; Heun, S. Josephson Diode effect in High-Mobility InSb Nanoflags. *Nano Lett.* **2022**, *22*, 8502.

(9) Golod, T.; Krasnov, V. M. Demonstration of a superconducting diode-with-memory, operational at zero magnetic field with switchable nonreciprocity. *Nat. Commun.* **2022**, *13*, 3658.

(10) Narita, H.; Ishizuka, J.; Kawarazaki, R.; Kan, D.; Shiota, Y.; Moriyama, T.; Shimakawa, Y.; Ognev, A. V.; Samardak, A. S.; Yanase, Y.; Ono, T. Field-free superconducting diode effect in noncentrosymmetric superconductor/ferromagnet multilayers. *Nat. Nanotechnol.* **2022**, *17*, 823.

(11) Pal, B.; Chakraborty, A.; Sivakumar, P. K.; Davydova, M.; Gopi, A. K.; Pandeya, A. K.; Krieger, J. A.; Zhang, Y.; Date, M.; Ju, S.; Yuan, N.; Schröter, N. B. M.; Fu, L.; Parkin, S. S. P. Josephson diode effect from cooper pair momentum in a topological semimetal. *Nat. Phys.* **2022**, *18*, 1228.

(12) Paolucci, F.; De Simoni, G.; Giazotto, F. A gate- and flux-controlled supercurrent diode effect. *Appl. Phys. Lett.* **2023**, *122*, No. 042601.

(13) Sundaresh, A.; Vayrynen, J. I.; Lyanda-Geller, Y.; Rokhinson, L. P. Diamagnetic mechanism of critical current non-reciprocity in multilayered superconductors. *Nat. Commun.* **2023**, *14*, 1628.

(14) Hou, Y.; Nichele, F.; Chi, H.; Lodesani, A.; Wu, Y.; Ritter, M. F.; Haxell, D. Z.; Davydova, M.; Ilić, S.; Glezakou-Elbert, O.; Varambally, A.; Bergeret, F. S.; Kamra, A.; Fu, L.; Lee, P. A.; Moodera, J. S. Ubiquitous Superconducting Diode Effect in Superconductor Thin Films. *Physics Review Letters* **2023**, *131*, No. 027001.

(15) Ghosh, S.; Patil, V.; Basu, A.; Kuldeep; Dutta, A.; Jangade, D. A.; Kulkarni, R.; Thamizhavel, A.; Steiner, J. F.; von Oppen, F.; Deshmukh, M. M. High-temperature Josephson diode. *Nat. Mater.* **2024**, 1.

(16) Wu, H.; Wang, Y.; Xu, Y.; Sivakumar, P. K.; Pasco, C.; Filippozzi, U.; Parkin, S. S. P.; Zeng, Y.-J.; McQueen, T.; Ali, M. N. The field-free Josephson diode in a van der Waals heterostructure. *Nature* **2022**, *604*, 653.

(17) Trahms, M.; Melischek, L.; Steiner, J. F.; Mahendru, B.; Tamir, I.; Bogdanoff, N.; Peters, O.; Reecht, G.; Winkelmann, C. B.; von Oppen, F.; Franke, K. J. Diode effect in Josephson junctions with a single magnetic atom. *Nature* **2023**, *615*, 628.

(18) Gupta, M.; Graziano, G. V.; Pendharkar, M.; Dong, J. T.; Dempsey, C. P.; Palmstrøm, C.; Pribiag, V. S. Gate-Tunable Superconducting Diode Effect in a Three-Terminal Josephson Device. *Nat. Commun.* **2023**, *14*, 3078.

(19) Chiles, J.; Arnault, E. G.; Chen, C. C.; Larson, T. F. Q.; Zhao, L. F.; Watanabe, K. J.; Taniguchi, T.; Amet, F.; Finkelstein, G. *Nano Lett.* **2023**, *23*, 5257−5263.

(20) Davydova, M.; Prembabu, S.; Fu, L. Universal Josephson Diode Effect. *Sci. Adv.* **2022**, *8*, eabo0309.

(21) Yu, K.; Heitmann, T. W.; Song, C.; DeFeo, M. P.; Plourde, B. L. T.; Hesselberth, M. B. S.; Kes, P. H. Asymmetric weak-pinning superconducting channels: Vortex ratchets. *Phys. Rev. B* **2007**, *76*, 220507.

(22) Palau, A.; Monton, C.; Rouco, V.; Obradors, X.; Puig, T. Guided vortex motion in YBa2Cu3O7 thin films with collective ratchet pinning potentials. *Phys. Rev. B* **2012**, *85*, No. 012502.

(23) Gutfreund, A.; Matsuki, H.; Plastovets, V.; Noah, A.; Gorzawski, L.; Fridman, N.; Yang, G.; Buzdin, A.; Millo, O.; Robinson, J. W. A.; Anahory, Y. Direct observation of a superconducting vortex diode. *Nat. Commun.* **2023**, *14*, 1630.

(24) Cerbu, D.; Gladilin, V. N.; Cuppens, J.; Fritzsche, J.; Tempere, J.; Devreese, J. T.; Moshchalkov, V. V.; Silhanek, A. V.; Van De Vondel, J. Vortex ratchet induced by controlled edge roughness. *New J. Phys.* **2013**, *15*, No. 063022.

(25) De Souza Silva, C. C.; Van De Vondel, J.; Zhu, B. Y.; Morelle, M.; Moshchalkov, V. V. Vortex ratchet effects in films with a periodic array of antidots. *Phys. Rev. B* **2006**, *73*, No. 014507.

(26) Shalóm, D. E.; Pastoriza, H. Vortex Motion Rectification in Josephson Junction Arrays with a Ratchet Potential. *Phys. Rev. Lett.* **2005**, *94*, 177001.

(27) de Souza Silva, C. C.; Van de Vondel, J.; Morelle, M.; Moshchalkov, V. V. Controlled multiple reversals of a ratchet effect. *Nature* **2006**, *440*, 651.

(28) Gillijns, W.; Silhanek, A. V.; Moshchalkov, V. V.; Reichhardt, C. J. O.; Reichhardt, C. Origin of Reversed Vortex Ratchet Motion. *Phys. Rev. Lett.* **2007**, *99*, 247002.

(29) Menghini, M.; Van De Vondel, J.; Gheorghe, D. G.; Wijngaarden, R. J.; Moshchalkov, V. V. Asymmetry reversal of thermomagnetic avalanches in Pb films with a ratchet pinning potential. *Phys. Rev. B* **2007**, *76*, 184515.

(30) De Souza Silva, C. C.; Silhanek, A. V.; Van De Vondel, J.; Gillijns, W.; Metlushko, V.; Ilic, B.; Moshchalkov, V. V. Dipole-Induced Vortex Ratchets in Superconducting Films with Arrays of Micromagnets. *Phys. Rev. Lett.* **2007**, *98*, 117005.

(31) Reichhardt, C.; Ray, D.; Reichhardt, C. J. O. Reversible ratchet effects for vortices in conformal pinning arrays. *Phys. Rev. B* **2015**, *91*, 184502.

(32) Lu, Q.; Reichhardt, C. J. O.; Reichhardt, C. Reversible vortex ratchet effects and ordering in superconductors with simple asymmetric potential arrays. *Phys. Rev. B* **2007**, *75*, No. 054502.

(33) Perez De Lara, D.; Erekhinsky, M.; Gonzalez, E. M.; Rosen, Y. J.; Schuller, I. K.; Vicent, J. L. Vortex ratchet reversal: Role of interstitial vortices. *Phys. Rev. B* **2011**, *83*, 174507.

(34) Milošević, M. V.; Peeters, F. M. Vortex pinning in a superconducting film due to in-plane magnetized ferromagnets of different shapes: The London approximation. *Phys. Rev. B* **2004**, *69*, 104522.

(35) Serrier-Garcia, L.; Timmermans, M.; Van de Vondel, J.; Moshchalkov, V. V. Pinning of superconducting vortices in MoGe/Au Thin nano-squares. *Physica C* **2017**, *533*, 109−113.

(36) Kwok, W. K.; Welp, U.; Glatz, A.; Koshelev, A. E.; Kihlstrom, K. J.; Crabtree, G. W. Vortices in High-Performance High-Temperature Superconductors. *Rep. Prog. Phys.* **2016**, *79*, 116501.

(37) Wang, Y. L.; Thoutam, L. R.; Xiao, Z. L.; Shen, B.; Pearson, J. E.; Divan, R.; Ocola, L. E.; Crabtree, G. W.; Kwok, W. K. Enhancing Superconducting Critical Current by Randomness. *Phys. Rev. B* **2016**, *93*, No. 045111.

(38) Lyu, Y.-Y.; Jiang, J.; Wang, Y.-L.; Xiao, Z.-L.; Dong, S.; Chen, Q.-H.; Milošević, M. V.; Wang, H.; Divan, R.; Pearson, J. E.; Wu, P.; Peeters, F. M.; Kwok, W.-K. Superconducting diode effect via conformal-mapped nanoholes. *Nat. Commun.* **2021**, *12*, 2703.

https://doi.org/10.1021/acs.nanolett.3c05008
Nano Lett. 2024, 24, 4108−4116

(39) Wang, Y.-L.; Ma, X.; Xu, J.; Xiao, Z.-L.; Snezhko, A.; Divan, R.; Ocola, L. E.; Pearson, J. E.; Janko, B.; Kwok, W.-K. Switchable Geometric Frustration in an Artificial-Spin-Ice-Superconductor Heterosystem. *Nat. Nanotechnol.* **2018**, *13*, 560.
(40) Villegas, J. E.; Savel'ev, S.; Nori, F.; Gonzalez, E. M.; Anguita, J. V.; Garcia, R.; Vicent, J. L. A Superconducting Reversible Rectifier That Controls the Motion of Magnetic Flux Quanta. *Science* **2003**, *302*, 1188.
(41) Villegas, J. E.; Gonzalez, E. M.; Gonzalez, M. P.; Anguita, J. V.; Vicent, J. L. Experimental ratchet effect in superconducting films with periodic arrays of asymmetric potentials. *Phys. Rev. B* **2005**, *71*, No. 024519.
(42) Rollano, V.; Muñoz-Noval, A.; Gomez, A.; Valdes-Bango, F.; Martin, J. I.; Velez, M.; Osorio, M. R.; Granados, D.; Gonzalez, E. M.; Vicent, J. L. Topologically Protected Superconducting Ratchet Effect Generated by Spin-Ice Nanomagnets. *Nanotechnology* **2019**, *30*, 244003.
(43) Krasnov, V. M.; Oboznov, V. A.; Pedersen, N. F. Fluxon Dynamics in Long Josephson Junctions in the Presence of a Temperature Gradient or Spatial Nonuniformity. *Phys. Rev. B* **1997**, *55*, 14486.
(44) Vávra, O.; Pfaff, W.; Monaco, R.; Aprili, M.; Strunk, C. Current-Controllable Planar S-(S/F)-S Josephson Junction. *Appl. Phys. Lett.* **2013**, *102*, No. 072602.
(45) Takiguchi, K.; Anh, L. D.; Chiba, T.; Shiratani, H.; Fukuzawa, R.; Takahashi, T.; Tanaka, M. Giant gate-controlled odd-parity magnetoresistance in one-dimensional channels with a magnetic proximity effect. *Nat. Commun.* **2022**, *13*, 6538.
(46) Moubah, R.; Magnus, F.; Hjörvarsson, B.; Andersson, G. Antisymmetric magnetoresistance in SmCo5 amorphous films with imprinted in-plane magnetic anisotropy. *J. Appl. Phys.* **2014**, *115*, No. 053911.
(47) Wang, Y.; Lee, P. A.; Silevitch, D. M.; Gomez, F.; Cooper, S. E.; Ren, Y.; Yan, J.-Q.; Mandrus, D.; Rosenbaum, T. F.; Feng, Y. Antisymmetric linear magnetoresistance and the planar Hall effect. *Nat. Commun.* **2020**, *11*, 216.
(48) Fujita, T. C.; Kozuka, Y.; Uchida, M.; Tsukazaki, A.; Arima, T.; Kawasaki, M. Odd-parity magnetoresistance in pyrochlore iridate thin films with broken time-reversal symmetry. *Sci. Rep.* **2015**, *5*, 9711.
(49) Albarakati, S.; Tan, C.; Chen, Z.-J.; Partridge, J. G.; Zheng, G.; Farrar, L.; Mayes, E. L. H.; Field, M. R.; Lee, C.; Wang, Y.; Xiong, Y.; Tian, M.; Xiang, F.; Hamilton, A. R.; Tretiakov, O. A.; Culcer, D.; Zhao, Y.-J.; Wang, L. Antisymmetric magnetoresistance in van der Waals Fe3GeTe2 /graphite/Fe3GeTe2 trilayer heterostructures. *Sci. Adv.* **2019**, *5*, eaaw0409.
(50) Krasnov, V. M. Junctions in a Local Inhomogeneous Magnetic Field. *Phys. Rev. B* **2020**, *101*, 144507.
(51) Libál, A.; Lee, D. Y.; Ortiz-Ambriz, A.; Reichhardt, C.; Reichhardt, C. J. O.; Tierno, P.; Nisoli, C. Ice rule fragility via topological charge transfer in artificial colloidal ice. *Nat. Commun.* **2018**, *9*, 4146.
(52) Ortiz-Ambriz, A.; Tierno, P. Engineering of frustration in colloidal artificial ices realized on microfeatured grooved lattices. *Nat. Commun.* **2016**, *7*, 10575.
(53) Ma, X.; Reichhardt, C. J. O.; Reichhardt, C. Reversible Vector Ratchets for Skyrmion Systems. *Phys. Rev. B* **2017**, *95*, 104401.
(54) Li, Q.; Stoica, V. A.; Pasciak, M.; Zhu, Y.; Yuan, Y.; Yang, T.; McCarter, M. R.; Das, S.; Yadav, A. K.; Park, S.; Dai, C.; Lee, H. J.; Ahn, Y.; Marks, S. D.; Yu, S.; Kadlec, C.; Sato, T.; Hoffmann, M. C.; Chollet, M.; Kozina, M. E.; Nelson, S.; Zhu, D.; Walko, D. A.; Lindenberg, A. M.; Evans, P. G.; Chen, L.-Q.; Ramesh, R.; Martin, L. W.; Gopalan, V.; Freeland, J. W.; Hlinka, J.; Wen, H. Subterahertz collective dynamics of polar vortices. *Nature* **2021**, *592*, 376.
(55) Geim, A. K.; Novoselov, K. S. The rise of graphene. *Nat. Mater.* **2007**, *6*, 183.

https://doi.org/10.1021/acs.nanolett.3c05008
Nano Lett. 2024, 24, 4108−4116